Supporting Information

Self-adaptive flexible valve as passive flow regulator

Qiang Zhang[1,2], Xirui Peng[1], Shayuan Weng[1,3], Rundong Zhang[4], Daining Fang[2,5], Ruike Zhao[4], H. Jerry Qi[1*]

[1]The George W. Woodruff School of Mechanical Engineering, Georgia Institute of Technology, Atlanta, GA 30332, USA

[2] State Key Laboratory for Turbulence and Complex System, College of Engineering, Peking University, Beijing, 100871, People's Republic of China

[3]College of Aerospace Engineering, Chongqing University, Chongqing, 400044, People's Republic of China

[4]Department of Mechanical and Aerospace Engineering, The Ohio State University, Columbus, OH 43210, USA

[5]Institute of Advanced Structure Technology, Beijing Institute of Technology, Beijing, 100081, People's Republic of China

Corresponding authors: HJQ: qih@me.gatech.edu.

Additional derivation process of the expressions in theoretical analysis

To obtain the expression of Eq. 7a and 7b in the main text, we first insert Eq. 6a into Eq. 5b and arrive at

$$\frac{d\omega}{ds}=\frac{qs\cos\alpha}{\kappa AG}+\sin\varphi\cos\alpha \tag{S1}$$

Inserting Eq. 6c into Eq. 5b, the following equation is obtained

$$qs=\kappa AG\left(\tan\alpha-\sin\varphi\right) \tag{S2}$$

Inserting the trigonometric relation $\frac{1}{\cos^2\alpha}=1+\tan^2\alpha$ and Eq. S2 into Eq. S1, we arrive at

$$\frac{d\omega}{ds}=\frac{qs}{\kappa AG\sqrt{\left(1+\left(\frac{qs}{\kappa AG}+\sin\varphi\right)^2\right)}}+\frac{\sin\varphi}{\sqrt{\left(1+\left(\frac{qs}{\kappa AG}+\sin\varphi\right)^2\right)}} \tag{S3}$$

We thus reproduce Eq. 7b in the main text. With Eq. 6a, the left-hand side of Eq. 5a can be further derived as

$$\begin{aligned}-EI\frac{d}{ds}\left(\cos\varphi\frac{d\varphi}{dx}\right)&=-EI\frac{d}{ds}\left(\cos\varphi\frac{d\varphi}{ds}\frac{ds}{dx}\right)=-EI\frac{d}{ds}\left(\frac{\cos\varphi}{\cos\alpha}\frac{d\varphi}{ds}\right)\\&=-EI\left(\frac{\cos\varphi}{\cos\alpha}\frac{d^2\varphi}{ds^2}+\frac{d\varphi}{ds}\frac{d}{ds}\left(\frac{\cos\varphi}{\cos\alpha}\right)\right)\end{aligned} \tag{S4}$$

Based on the first-order approximation, the second term on the right-hand side of Eq. S4 can be ignored compared with the first term. Therefore, Eq. 5a can be approximately rewritten as

$$-EI\frac{\cos\varphi}{\cos\alpha}\frac{d^2\varphi}{ds^2}=qs\cos\alpha \tag{S5}$$

Inserting the trigonometric relation $\frac{1}{\cos^2\alpha}=1+\tan^2\alpha$ and Eq. S2 into Eq. S5, we arrive at

$$\frac{d^2\varphi}{ds^2}=-\frac{qs}{EI\cos\varphi\left(1+\left(\frac{qs}{\kappa AG}+\sin\varphi\right)^2\right)} \tag{S6}$$

We thus reproduce Eq. 7a in the main text. At the free end of the cantilever beam (Fig. 2c, $s=0$), there is no bending moment and thus the first derivation of φ at this point is zero ($\varphi'\left(s=0\right)=0$). While for the clamped end (Fig. 2c, $s=l$), both the angular displacement and deflection displacement are zero. Therefore,

we have the boundaries $\varphi(s=l)=0$ and $\omega(s=l)=0$. To solve Eq. 7a and 7b, relations $A=W_{flap}t$, $I=W_{flap}t^3/12$, and $W_{flap}\approx W$ are used (The definitions of these variables can be found in the main text). After solving the equations, we can obtain the deflection of the flap tip ω_{tip}, the rotation angle of the flap end φ_{tip}, and the horizontal displacement of the center point at the flap end u_{tip}, for different levels of pressure. To further obtain the expression of d, we can use the geometry relations that relate the deformed configuration of the flap to its initial undeformed configuration. As shown in Figure S1, the line AB in the initial undeformed configuration becomes $A'B'$ after deformation. According to the calculated deflection results, the length of AC and $A'C$ is ω_{tip} and u_{tip}, respectively, while the angle of $\angle EA'B'$ is φ_{tip}. Therefore, the length of BD and $B'D$ shown in Figure S1 can be easily computed as $\left(\omega_{tip}+\frac{t}{2}\cos\varphi_{tip}-\frac{t}{2}\right)$ and $\left(u_{tip}+\frac{t}{2}\sin\varphi_{tip}\right)$, respectively. The length of BB' can be obtained based on the length of BD and $B'D$ through Pythagorean theorem. Following the simple geometry relations marked in the red line in Figure S1, the expression of d can be written as

$$d=d_0-\cos\left(\theta+\tan^{-1}\left(\frac{u_{tip}+\frac{t}{2}\sin\varphi_{tip}}{\omega_{tip}+\frac{t}{2}\cos\varphi_{tip}-\frac{t}{2}}\right)\right)\times\sqrt{\left(u_{tip}+\frac{t}{2}\sin\varphi_{tip}\right)^2+\left(\omega_{tip}+\frac{t}{2}\cos\varphi_{tip}-\frac{t}{2}\right)^2} \tag{S7}$$

where θ is the tilt angle of the flap relative to the top channel wall, d_0 is the initial gap between the flap tip and the bottom channel wall, t is the thickness of the flap, respectively.

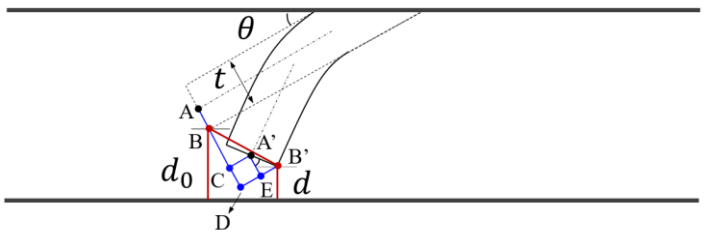

Figure S1. Schematic graph of the geometry relations that relate the deformed configuration of the flap to its initial undeformed configuration.

Geometry and fabrication of the valves

To manufacture the valves, we build a digit light processing printing platform as schematically shown in Figure S2a. It is mainly composed of an ultraviolet (UV) light projector and a linear translation stage. The operation of the platform is controlled by a MATLAB script. In Figure S2b, we show the geometry of a typical valve used for characterizing the flow rate-pressure response. The length of the main channel is 22 mm. Both the width and height of the channel is 1 mm. To connect the channel into a testing system, we also add a cylindrical inlet and outlet on the two sides of the channel. Both the length and diameter of the inlet and outlet is 4 mm.

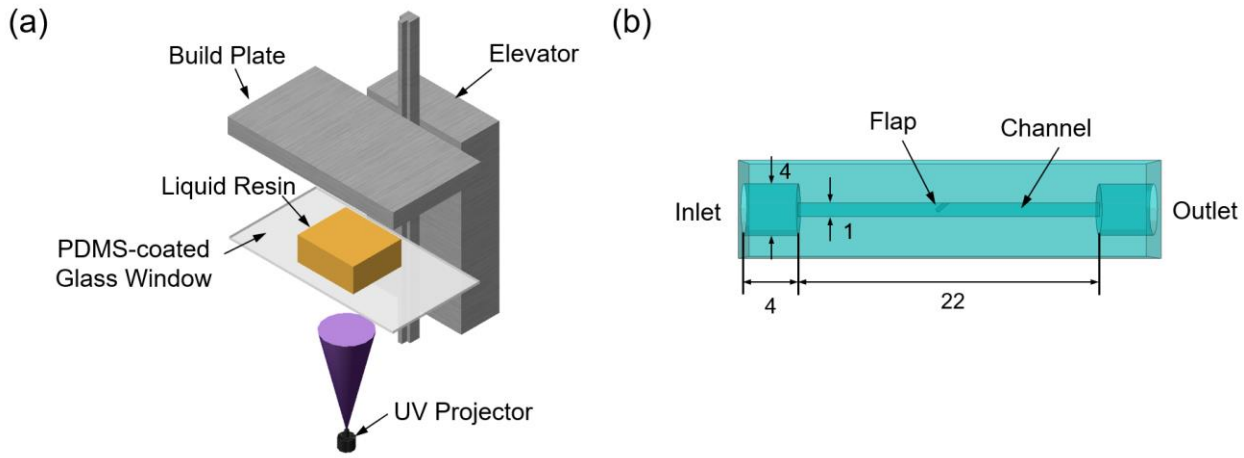

Figure S2. Geometry and fabrication of the valves. (a) Schematic graph of the printing platform. (b) Geometry of the valve used for charactering the flow rate-pressure response. Number unit: mm.

Mechanical properties of the material

For modeling the mechanical behavior of the flap in simulations, a neo-Hookean material model is used. In order to determine the material parameters in the model, tensile tests are performed and the stress-strain curve for the material is extracted in Figure S3. In terms of principal stretches, the strain energy density function for an incompressible neo-Hookean material is given by

$$W = C_1\left(\lambda_1^2 + \lambda_2^2 + \lambda_3^2 - 3\right);\ \lambda_1\lambda_2\lambda_3 = 1 \tag{S8}$$

where λ_i $(i = 1,2,3)$ are the principal stretches and C_1 is a material-specific parameter. The expressions for the Cauchy stress differences is given as

$$\sigma_{11} - \sigma_{33} = 2C_1\left(\lambda_1^2 - \lambda_3^2\right) \tag{S9}$$

In the case of simple tension, $\sigma_{33}=0$ and $\lambda_2=\lambda_3=1/\sqrt{\lambda}$. Eq. S9 can be written as

$$\sigma_{11}=2C_1\left(\lambda^2-\frac{1}{\lambda}\right) \tag{S10}$$

Figure S3 presents the best fitting model curve of Eq. S10 with parameter values $C_1=0.3167\,\mathrm{J/m^3}$.

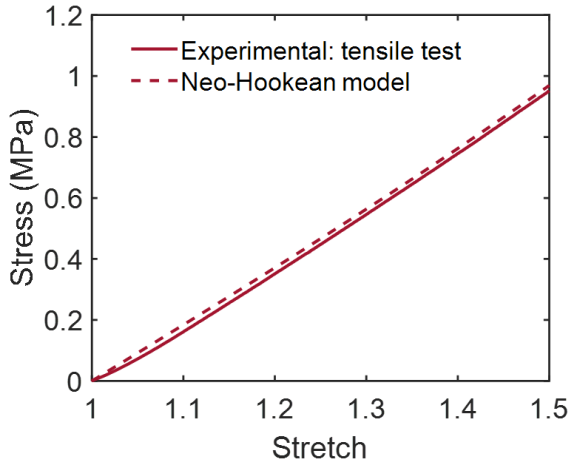

Figure S3. Neo-Hookean constitutive model stress-strain curve against the corresponding experimental data.

Table S1. List of parameters used in the theoretical and numerical models

Parameters	Notation	Value
Elastic modulus	E	2.0 MPa
Timoshenko shear coefficient	κ	5/6
Lumped friction coefficient	η	0.75
Density of water	ρ_{water}	1.0×10^3 kg/m^3
Viscosity of water	η_{water}	8.9×10^{-4} Pa s
Shear modulus	G	0.67 MPa
Density of polymer	ρ_{polymer}	~ 1.19×10^3 kg/m^3